Numerical simulation of cooling performance of radiant ceiling system interacting with a ceiling fan

Xingguo Guo[a], Shuangshuang Wan[a], Wenhua Chen[a,*], Hui Zhang[b], Edward Arens[b], Yuanda Cheng[c], Wilmer Pasut[d,e]

[a] School of Infrastructure Engineering, Nanchang University, Nanchang, China

[b] Center for the Built Environment, University of California, Berkeley, CA, USA

[c] College of Civil Engineering, Taiyuan University of Technology, Taiyuan, China

[d] Universita' Ca' Foscari, Venezia, Italy

[e] Department of Architecture, Korea University, Seoul, South Korea

[*] *Corresponding author: chenwenhua14@tju.edu.cn*

Abstract: We evaluate the heat transfer from radiant ceilings that have suspended acoustical panels present for noise reduction. An upward-directed ceiling fan is added to offset the reduction of heat exchange due to the acoustical panels. We systematically simulate the indoor thermal environment and the changes to heat transfer coefficients caused by the interaction between radiant ceiling panels, acoustical panels, and ceiling fan under four influencing factors: (1) coverage ratio of acoustical panels, (2) fan rotational speed, (3) radiation panel temperature and (4) room height. The simulation method is validated with experimental data. Numerical results show that the augmented air speed increases convective and total heat transfer for radiant panel. Simulated temperature non-uniformity, air and operative temperature in the occupied part of the room is reduced with increased fan speed, and with decreased acoustical panel coverage ratio. The PMV increased with increased acoustical panel coverage ratio and radiant surface temperature, and also with reduced fan speed. When using fans, the radiant surface temperature can be raised 2 ℃ while maintaining equivalent thermal comfort, allowing higher water supply temperatures. The radiation heat transfer coefficient of the bare ceiling is decreased 25% by adding 63% acoustical panel coverage. The total heat transfer coefficient of radiant ceiling increases with fan speed up to 106.2% over a no-fan base case, and decreases with increased acoustical panel coverage ratio. The study indicates that an upward-directed ceiling fan is a worthwhile method to enable raised radiant surface temperatures, save cooling energy, and reduce surface condensation risk.

Keywords: Radiant system; Acoustical panels; Ceiling fan; Thermal environment; Heat transfer coefficients; CFD

doi.org/10.1016/j.enbuild.2023.113492
escholarship.org/uc/item/0w2289kw

Nomenclature

h_c Convective heat transfer coefficient (W m^{-2} K^{-1})	ε Emissivity (–)
h_r Radiant heat transfer coefficient (W m^{-2} K^{-1})	t_a Air temperature (℃)
h_{total} Total heat transfer coefficient (W m^{-2} K^{-1})	t_j j-surface temperature (℃)
t_{AUST} Average unheated surface temperature (℃)	t_s Radiant surface temperature (℃)
q_c Convective heat flux density (W m^{-2})	$A_{unshaded}$ Unshaded area of surface (m^2)
q_r Radiant heat flux density (W m^{-2})	A_{total} Total area of surface (m^2)
q_{total} Total heat flux density (W m^{-2})	A_{shaded} Shaded area of surface (m^2)
PMV Predicted Mean Vote	PD Predicted draft sensation (%)
U_{CC} Cooling capacity coefficient (W m^{-2} K^{-1})	t_{op} Operative temperature (℃)
M Human metabolic rate of thermogenesis (W m^{-2})	t_{mr} Mean radiant temperature (℃)
W Effective mechanical power (W)	$t_{w,m}$ Mean water temperature (℃)
f_{cl} A factor of clothing surface area (clo)	T_u Turbulence intensity (%)
t_{cl} clothing surface temperature (℃)	V Air speed (m/s)
F_{s-j} View factor between radiant surface and j-surface	P_a the steam partial pressure (Pa)

$Q_{12,\ shield}$ Radiative heat transfer between surface 1 and surface 2 with the shield (W)

$Q_{12,\ unshield}$ Radiative heat transfer between surface 1 and surface 2 without the shield (W)

$Q_{t,\ shield}$ Heat transfer of the ceiling partially shielded by the acoustical panels (W)

1 Introduction

In 2021 the operation of buildings accounted for 30% of global final energy consumption [1, 2]. HVAC energy conservation has become one of the most important goals in the field of building energy saving [3]. In recent years, the use of radiant cooling system is increasing due to the higher energy efficiency compared with all-air systems [4-6].

However, the high acoustical reflectivity of the concrete exposed on the radiant surfaces of ThermoActive Building Systems (TABS) causes noise problems [4]. Free-hanging acoustical panels can be used to achieve acceptable sound absorption and maintain a good acoustic quality in the space [7]. However, acoustical panels can reduce the cooling capacity of radiant ceilings [7-9] and have a negative effect on the indoor thermal environment [7, 10, 11]. Weitzmann et al. [8] established a cooling capacity coefficient equation, and found that an 80% coverage of suspended acoustical panels reduced the cooling capacity coefficient of a TABS by 30%. Karmann et al. [7] found the cooling capacity coefficient reduced by 11% with an acoustical panel coverage of 47%. Domínguez et al. [9] compared the influence of

doi.org/10.1016/j.enbuild.2023.113492
escholarship.org/uc/item/0w2289kw

two kinds of acoustical panels on the TABS cooling performance. The cooling capacity coefficient was reduced by 36% and 14% with 80% coverage of horizontal and vertical acoustical panels respectively. These were accompanied by room operative temperature increases of 1.6 ℃ and 1.1 ℃ respectively. In addition, field studies of acoustical panels [10, 11] report increments in operative temperature of 1-2 ℃.

Hence, free-hanging acoustical panels have negative effects on the radiant ceiling system performance. The heat transfer of the radiant system could be enhanced by increasing its convective component [12]. Ning et al. [13] studied the impact of forced convection on the cooling capacity of radiant ceiling panels, finding that forced convection increased capacity by 43-46% in comparison to the radiation system only. Another experimental test [14] studied the impact of a high aspiration diffuser on the heat fluxes of a radiant ceiling system, finding the convective heat transfer of radiant ceiling panels near a high aspiration diffuser to be increased by 4-17 %. Ye et al. [15] investigated the heat flux changes of radiant cooling ceiling panels interacting with a wall-attached jet, finding that forced convection increased heat transfer with increased supply air speed. Kim et al. [16] united airbox convectors with a radiant ceiling panel, found that the capacity of the cooling system increased by 3.2% at a fixed chilled water flowrate. With the cooling energy consumption of the united system was reduced 6.3% compared to the radiant system alone [16]. Zhao et al. [17] reported that a more comfortable indoor thermal environment could be obtained via combining radiant ceiling and mixed ventilation rather than using radiant cooling system alone. Choi et al. [18] determined the impact of an air circulator with DC fans on the cooling capacity of an open-type radiant cooling system. Choi et al. [18] found the cooling capacity of the radiant ceiling can increase up to 16-22% in comparison to the radiant system only.

In general, these above studies [13-17] indicate that the cooling performance and thermal comfort from radiant ceiling systems can be improved by increasing convection. Compared with conventional mixing convection caused by a room ventilation system and/or natural convection [13-17], the air circulation from ceiling fans has a larger effect on convective heat transfer because ceiling fan air speed is typically higher than that created by ventilation systems. It is also typically more energy efficient [19].

Surveys in buildings [20-22] have found that occupants generally prefer higher air speeds in typical air-conditioned environments. The elevated air movements around occupants caused by ceiling fans can compensate up to 4 ℃ of indoor air temperature for equivalent thermal comfort [21, 23, 24]. Thus, a ceiling-fan-integrated radiant system cools occupants both via surface temperatures in the room and directly by increased convection from the skin to room air. Karmann et al. [25] experimentally studied the effect of an upward-directed ceiling fan on the cooling capacity of a radiant ceiling with acoustical panels. They [25] found the cooling capacity can increase up to 22% with ceiling fan in comparison to the case without fan. Nevertheless, the impacts of acoustical panels and ceiling fan on heat transfer coefficients and thermal comfort need further description, because the study only

doi.org/10.1016/j.enbuild.2023.113492
escholarship.org/uc/item/0w2289kw

covers a limited number of test conditions.

This paper aims to provide generalizable knowledge for design, and optimization of the coupling operation parameters of ceiling-fan-integrated radiant ceiling cooling systems. This simulation study systematically investigates the indoor thermal environment and heat transfer coefficient changes of radiant ceiling system interacting with a ceiling fan under different influencing factors including: (1) coverage ratio of acoustical panel, (2) fan rotational speed, (3) radiant surface temperature and (4) room height. The simulation method was first validated using experimental data, and then employed to determine the above-mentioned factors.

2 Method

2.1 Geometry and CFD simulation

The size of the simulated office is 4.27 m × 4.27 m × 2.50 m. The simulated office is without windows, the wall and the floor is approximately an adiabatic boundary. The total heat load of the simulation is fixed at 1097 W. As shown in Fig. 1, the heat sources in the simulations include four computers (300 W, 16.5 W m^{-2}), four screens (283 W, 15.5 W m^{-2}), four lights (214 W, 11.8 W m^{-2}) and four occupants (300 W, 16.5 W m^{-2}). A fixed heat flux was set as the boundary condition of these heat sources. Room geometry, internal loads, and parameters of the radiant panel and acoustical panel are the same as those described in the lab tests [25], because the test data were used to validate the simulation method of this study. The radiant panels are centered on the ceiling (Fig. 1). The coverage ratio of the radiant panels is 73.5%, with an area of 13.4 m^2. In order to simplify the geometry model, the cold-water circulation pipes of the radiant ceiling were not directly modeled. Since the mean cold-water temperature was kept constant in the tests [7, 25], as an approximate method [18] the radiant ceiling surface is simulated at a fixed temperature. Fig. 2 shows the four coverage ratios of the acoustical panel. The total ceiling area (not the radiant panel area) is used as the base value to calculate the acoustical panel coverage. The ceiling fan was mounted at 25 cm below the ceiling surface and blowing upward. Due to the upward-directed ceiling fan can bring a higher cooling capacity of the radiant cooling ceiling than the downward-directed ceiling fan [25]. The diameter of the ceiling fan is 132 cm. Since the power of fan is only 6 W [25], this heat load was ignored.

Grid independence tests were conducted using 0.7, 1.1 and 1.5 million grid cells to compare simulated velocity and temperature profiles (see Fig. 3). Fig. 3 shows that the medium grid (1.1 million) produced a negligible difference in comparison to the fine grid (1.5 million). Therefore, medium grids were applied in the simulations. The largest skewness of the medium grid is 0.84. The grid size growth rate is 1.2.

The simulations were conducted as steady-state calculations. The Realizable k-ε model [26, 27] was employed to investigate turbulent airflow. This turbulence model is commonly used for medium intensity swirling-flow. The radiant heat transfer in the office was calculated by the surface-to-surface (S2S) model [15, 28]. The Boussinesq hypothesis was utilized to solve the natural convection phenomenon to reflect the change of air density with temperature. The second-order upwind scheme was utilized

doi.org/10.1016/j.enbuild.2023.113492
escholarship.org/uc/item/0w2289kw

to discretize the governing equations. The SIMPLE algorithm [15, 28] was used to solve the discrete equations. The solver was set to an implicit scheme based on pressure. The rotating motion of ceiling fan was simulated by the multiple reference frame (MRF) method [27].

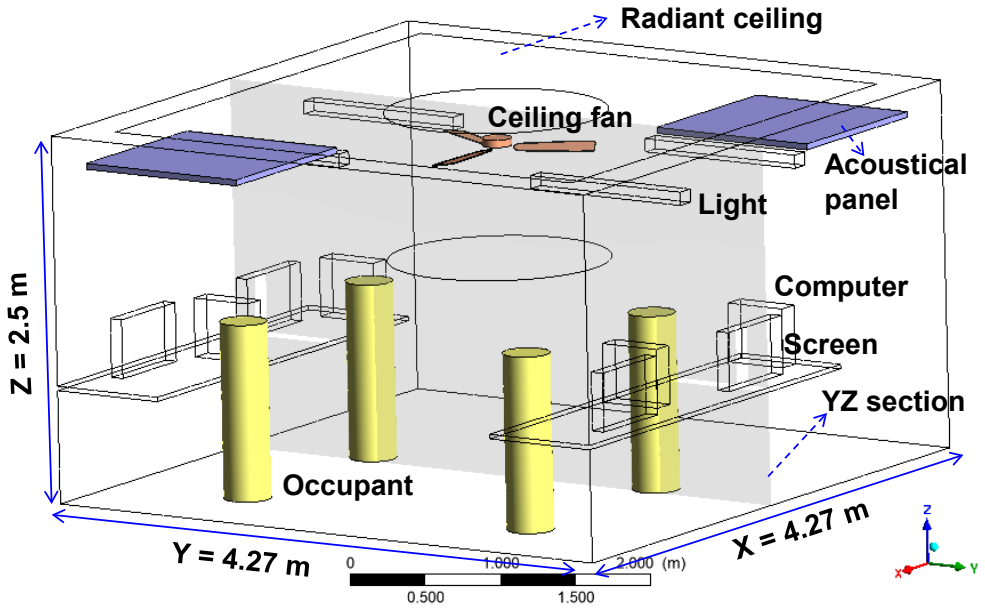

Fig. 1. Geometry for the CFD simulation.

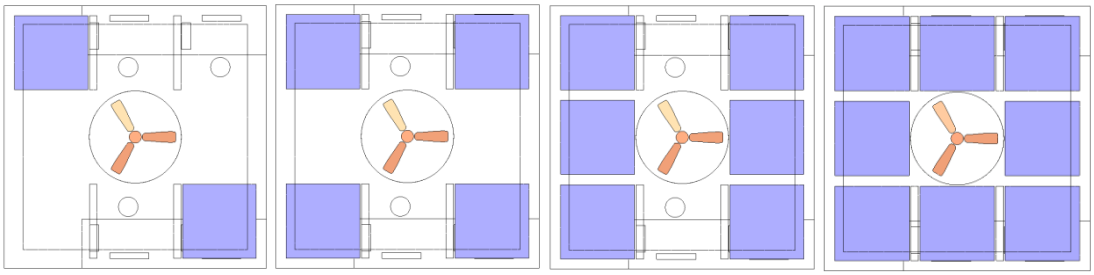

16% coverage ratio 32% coverage ratio 47% coverage ratio 63% coverage ratio

Fig. 2. Layout of acoustical panels.

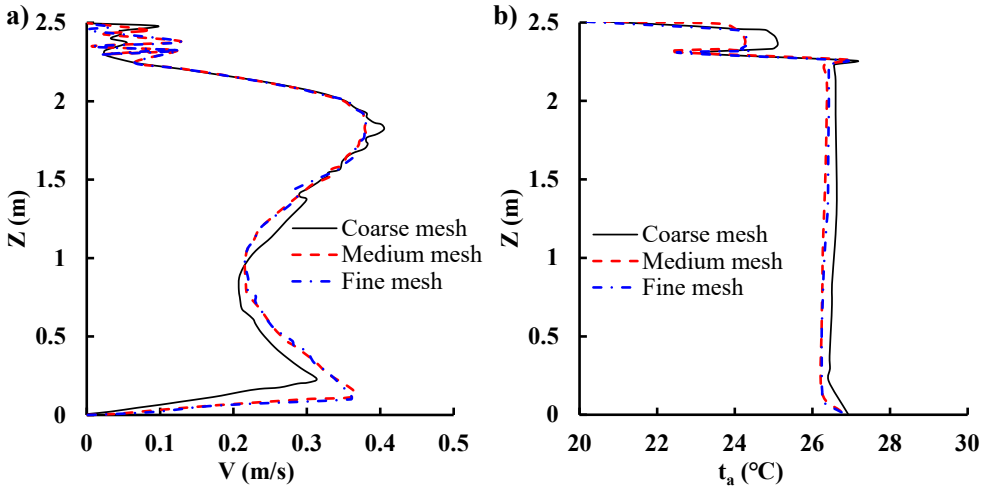

Fig. 3. a) air velocity and b) temperature profiles for different grid sizes in the vertical centerline of the room.

doi.org/10.1016/j.enbuild.2023.113492
escholarship.org/uc/item/0w2289kw

This study analyzed the impact of four different factors on this combined system, including the coverage ratio of acoustical panels, fan rotational speed (S), radiant surface temperature (t_s) and room height (H). Table 1 lists the simulated cases.

Table 1. Sequence of simulated cases.

Series	Case	Acoustic panel coverage (%)	Fan	S (rpm)	t_s (°C)	H (m)
A	A1-A5	0、16、32、47、63	No fan	/	20.6	2.5
B	B1-B5	0、16、32、47、63	Fan upward	73	20.6	2.5
C	C1-C5			146		
D	D1-D5			219		
E	E1-E5	0、16、32、47、63	Fan upward	146	18.6	2.5
F	F1-F5				19.6	
G	G1-G5				21.6	
H	H1-H5				22.6	
I	I1-I5	0、16、32、47、63	Fan upward	146	20.6	3
J	J1-J5					4

2.2 Thermal comfort indexes

PMV and PD index [29] were applied to estimate the thermal comfort in the occupied zone. PMV can be calculated by equation (1) [29, 30].

$$PMV = \left[0.303\exp\left(-0.036M\right)+0.0275\right] \times \begin{Bmatrix} \left(M-W\right) \\ -3.05\left[5.733-0.007\left(M-W\right)-P_a\right]-0.42\left(M-W-58.15\right) \\ -1.73\times10^{-2}M\left(5.867-P_a\right)-1.4\times10^{-3}M\left(34-t_a\right) \\ -3.96\times10^{-8}\times f_{cl}\left[\left(t_{cl}+273\right)^4-\left(t_{mr}+273\right)^4\right]-f_{cl}h_c\left(t_{cl}-t_a\right) \end{Bmatrix} \quad (1)$$

The M and clothing value f_{cl} was set as 1.0 Met and 0.7 clo in the PMV model, respectively. The relative humidity of air was set as 50%. PD was calculated by equation (2) [29].

$$PD = \left(34-t_a\right)\left(V-0.05\right)^{0.62}\left(0.37V\bullet T_u+3.14\right) \quad (2)$$

Our previous study [19] has shown that the velocity fields driven by ceiling fans are non-uniform, with higher flows near the floor. Thus, 0.1 m height is applied as the first simulation point because of the draft sensation at ankle height.

2.3 Heat transfer coefficients determination

t_{AUST} is applied as the reference temperature to determine the h_r [24]. t_{AUST} can be calculated by equation (3) [31].

$$t_{AUST} = \sqrt[4]{\sum_{j=1}^{n}\left(F_{s-j}(t_j+273)^4\right)}-273 \quad (3)$$

Equation (4) is used to determine the h_r from the radiant ceiling [32].

doi.org/10.1016/j.enbuild.2023.113492
escholarship.org/uc/item/0w2289kw

$$h_r = \frac{q_r}{t_{AUST} - t_s} \tag{4}$$

The air temperature at 1.1 m height ($t_{a1.1}$) in the office is applied as the reference temperature to determine the h_c [32]. The operative temperature at 1.1 m height ($t_{op1.1}$)is applied as the reference temperature to determine the h_{total} [32]. Then, 1.1 m height is applied as the second simulation point because of the draft sensation at the head/neck for a seated person [33]. Considering the effect of air movement driven by the ceiling fan, t_{op} is expressed as [25]:

$$t_{op} = \frac{t_{mr} + \left(t_a \bullet \sqrt{10V}\right)}{1 + \sqrt{10V}} \tag{5}$$

The t_{mr} is derived from the t_{AUST} by the following equation [30]:

$$t_{mr} = t_{AUST} - 2 \tag{6}$$

The h_{total} from the radiant ceiling was calculated using equation (7) [32].

$$h_{total} = \frac{q_{total}}{t_{op} - t_s} \tag{7}$$

The q_{total} and q_r from the radiant ceiling is directly calculated according to the simulation results. The q_c can be calculated by equation (8) [32].

$$q_c = q_{total} - q_r \tag{8}$$

The h_c from the radiant ceiling is determined by equation (9) [32].

$$h_c = \frac{q_c}{t_a - t_s} \tag{9}$$

2.4 Cooling capacity coefficient determination

Under steady state conditions, the U_{cc} of the radiant ceiling is determined by equation (10) [25]:

$$U_{cc} = \frac{q_{total}}{t_{op} - t_{w,m}} \tag{10}$$

It should be noted that the U_{cc} is only used to validate the numerical modeling,

doi.org/10.1016/j.enbuild.2023.113492
escholarship.org/uc/item/0w2289kw

since water is not simulated in radiant systems. The $t_{w,m}$ for cases C was set at 17.1 ℃, the same as the experimental study [25].

3. Results

3.1 Validation of numerical modeling

The simulation method was first validated via the experimental data of reference [25]. Fig. 4 compares the CFD simulated data (cases C, Table 1) with the measured t_a at 1.1 m height in the room centerline and cooling capacity coefficient. The simulated air temperature is slightly larger than the experimental data, As shown in Fig. 4a. The difference is within 5%, which is almost negligible. The curve slope obtained by CFD simulation is consistent with the curve slope obtained by experiment. Fig. 4b shows that the simulated data of cooling capacity coefficient change rate is consistent with the measured results. The maximum deviation between the simulated value and the experimental value of the cooling capacity coefficient change occurs when the acoustical panel coverage is 63%, and the deviation is 5%. In general, the experimental air temperatures and change in cooling capacity coefficient from [25] are all well presented by the CFD simulations. It suggests that the complex airflow of this study can be predicted well by the numerical methods applied in this study.

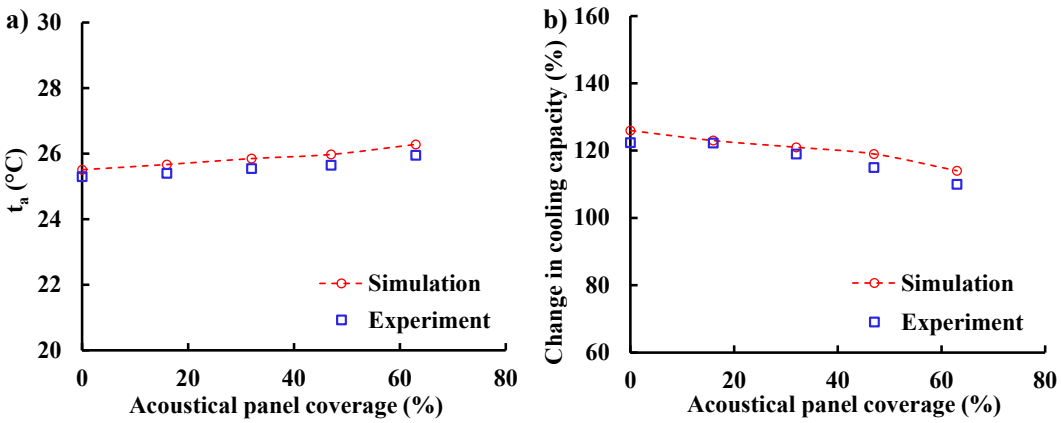

Fig. 4. Comparisons between the experimental and numerical a) air temperature at 1.1 m height and b) change in cooling capacity coefficient for Cases C.

3.2 Indoor environmental

3.2.1 Air velocity and temperature

Fig. 5 illustrates the velocity fields of Series A-D (see Table 1) for a section plane YZ (see Fig. 1) acquired in the middle of the office. Each row depicts a series at one fan rotational speed (fan off and fan at 3 different rotation speeds). Each column represents one acoustical panel coverage ratio (zero coverage and 4 different coverages). The air velocity distributions for all cases are almost symmetrical in the YZ section due to the symmetry of the geometry model and heat load. It can be observed that without the ceiling fan running (see first row in Fig. 5), air speeds for all

the acoustical panel coverage ratios are smaller than 0.3 m/s. The first row also shows that without ceiling fan, the acoustical panel coverage ratios have insignificant effect on the airflow pattern.

With the fan running, the airflow patterns with an upward-running ceiling fan are transformed into a ceiling-attached jet due to the Coanda effect and to the presence of the acoustic panels. This airflow layer near the ceiling helps to augment the heat exchange from the radiant ceiling. It can be shown by the reduced ambient temperatures and PMV values (Figs 6 – 8 below). In section plane YZ, the airflow patterns are dominated by the upward ceiling fan airflow. The five columns show a similar flow pattern in spite of different acoustical panel coverages. In fact, all the airflow patterns are similar with the different acoustical panel coverages and the fan rotation speeds. While, the air velocity magnitudes increase with the fan rotation speed increases (rows 2-4 in Fig. 5). Cases B, C, D all with the highest speed near the floor. In the occupied area, the average air velocity magnitude for Cases B, C, D is below 0.3, 0.5 and 0.8 m/s, respectively. Unlike the downward-running ceiling fan [19], the upward-directed ceiling fan helps to construct a relatively uniform flow distribution in the occupied area. In general, the air speed is below the upper limit value for air movement without personal control (0.8 m/s) in the occupied area [24]. Regarding Fig. 5, it indicated that the air movements elevated by the upward ceiling fan has an insignificant influence on draft risk by the occupants.

Fig. 6 illustrates the air temperature fields of Series A-D in the YZ section. Similar to the above velocity fields, the air temperature fields in the YZ section for cases A-D are almost symmetrical. Unlike the velocity distribution, the first row shows that the acoustical panel coverage ratios have noteworthy impacts on the air temperature distributions without ceiling fan. The air temperature in the YZ section increases as the acoustical panel coverage ratio increases. This occurs due to the reduction of radiant heat exchanges from the radiant ceiling with increasing the acoustical panel coverage ratio. According to Fig. 6, this phenomenon also exists for the case B when the fan rotation speed is low (73 rpm). When the fan at 146 and 219 rpm, the higher panel coverage ratios saw less air temperature growth.

Besides, Fig. 6 depicts the air temperature uniformity in agreement with the fan rotational speed. The first row in Fig. 6 shows obvious temperature stratification in the YZ section for the case without fan. The temperature non-uniformity is reduced with increasing fan speed. In the YZ section, the vertical temperature stratification for case A is approximately 2.5 ℃, while for case D it is within 0.5 ℃. It reveals that the upward ceiling fan can be used to counteract stratification. The four rows in Fig. 6 present the reduction of air temperature variation with increasing the fan speed. It is due to the higher fan speed leading to a higher air mixing. In the occupied zone, an upward-directed ceiling fan reduces the average temperature by 2-6 ℃ depending on the fan speed, compared to the no-fan condition. Regarding Fig. 5 and Fig. 6, it can be inferred that the addition of upward ceiling fan into the radiant ceiling not only can be used to elevate air movement which can cool the occupants, and increase heat transfer which can reduce the ambient air temperature, but also make the indoor air temperature more uniform.

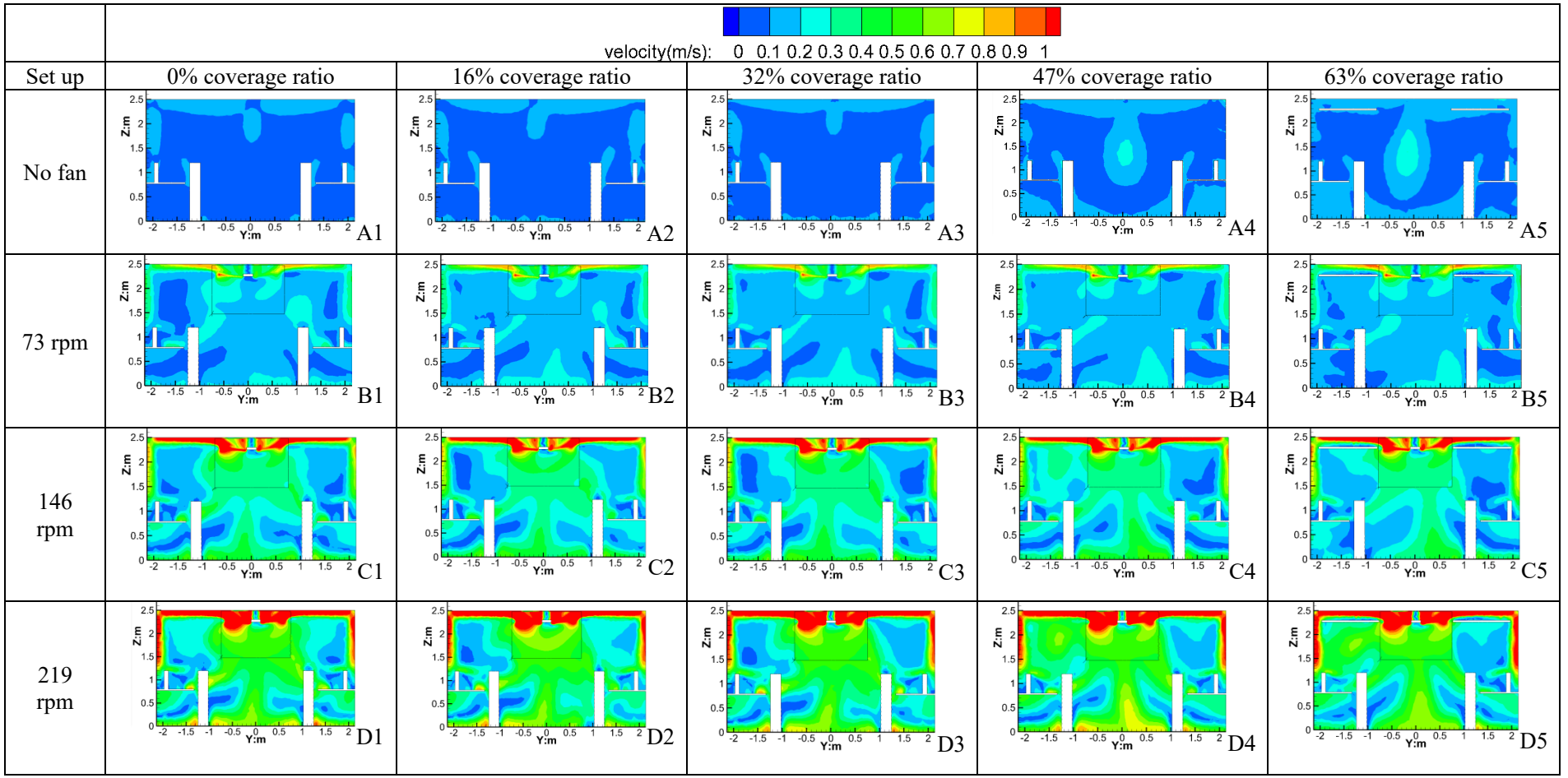

Fig. 5. Air velocity fields of Series A-D in the YZ section. Simulation conditions are described in Table 1.

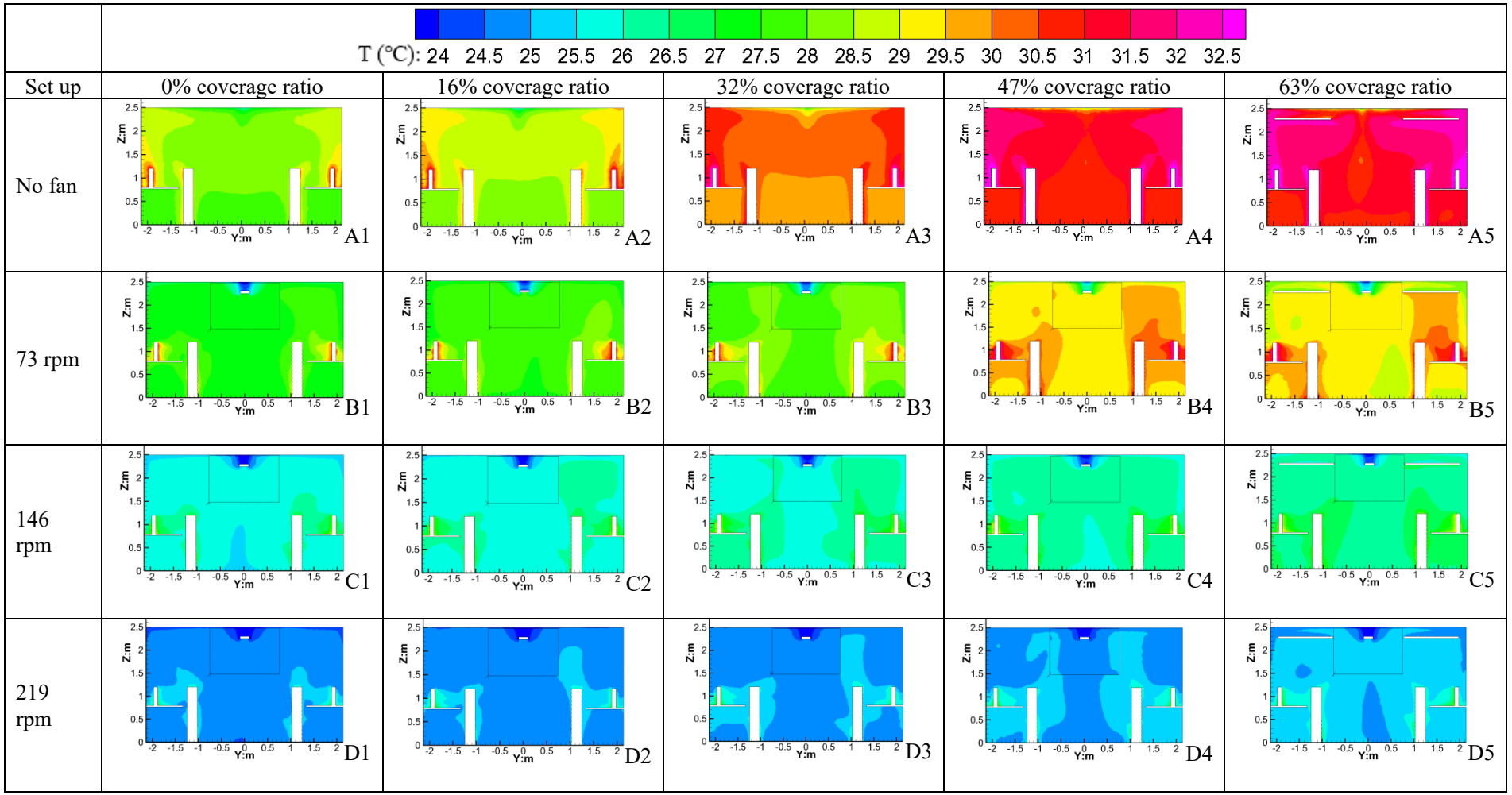

Fig. 6. Air temperature fields of Series A-D in the YZ section.

Fig. 7 a-c delineate the average air speeds at 0.1 m height versus the coverage ratio of acoustical panels for different fan rotational speed, radiant surface temperature and room height. Fig. 7 d-f and Fig. 7 g-i present the average t_a and t_{op} at 1.1 m height versus the coverage ratio of acoustical panels for different conditions, respectively. For the influence of fan rotational speed, Fig. 7a shows that the air speed is augmented with the fan speed, while Fig. 7d and Fig. 7g show that the t_a and t_{op} are both reduced with the fan speed respectively, indicating increased heat exchange with the radiant ceiling. Compared to the base case without fan, the decrement of t_a and t_{op} with fan at the highest fan rotation speed (219 rpm) is up to 3.8-6.2 ℃ and 3.54-6.1 ℃, respectively. Fig. 7b shows that the radiant surface temperature plays no role in the velocity. The average t_a and t_{op} are both increased with radiant surface temperature (Fig. 7e), and the t_a and t_{op} increment are both close to the increment of radiant surface temperature due to the walls which are set as adiabatic boundaries. Fig. 7c illustrates that the average air speed at 0.1 m height is reduced about 0.1 m/s with the room height increased from 2.5 m to 4 m, while Fig. 7f and Fig. 7i show that the average t_a and t_{op} both have a very slight increase with the room height increases from 2.5 m to 4 m. In general, Fig. 7 illustrates that the fan speeds have stronger impacts on the air velocity and temperature compared to the room height.

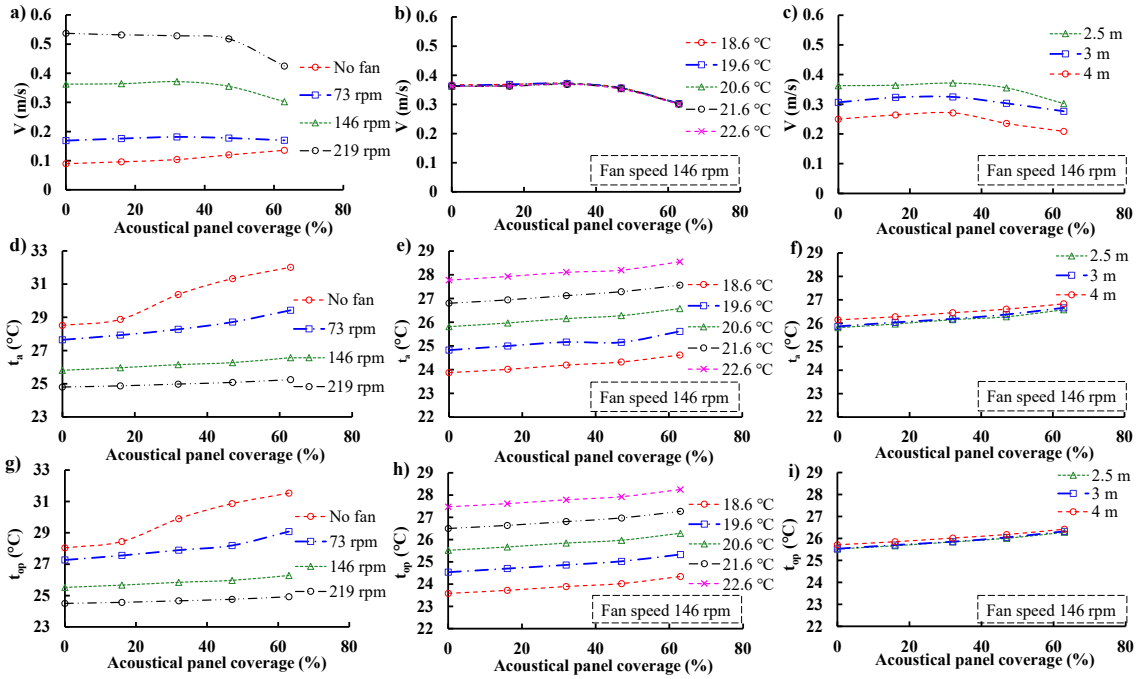

Fig. 7. a) - c) Average air velocity simulated over a hypothetical horizontal plan placed at 0.1 m height for different conditions shown in Table 1, d) - f) average air temperature at 1.1 m

height for different conditions shown in Table 1. g) - i) average operative temperature at 1.1 m height for different conditions shown in Table 1.

Fig. 8 a-c delineate the difference between average air and operative temperature at 1.1 m height versus the coverage ratio of acoustical panels for different fan rotational speed, radiant surface temperature and room height. The difference is within 0.25-0.5 ℃ for all cases. For the influence of fan rotational speed, Fig. 8a shows that the difference is reduced with the fan speed, while Fig. 8c shows that the difference is augmented with the room height. Fig. 8b shows that the radiant surface temperature plays no role in the difference.

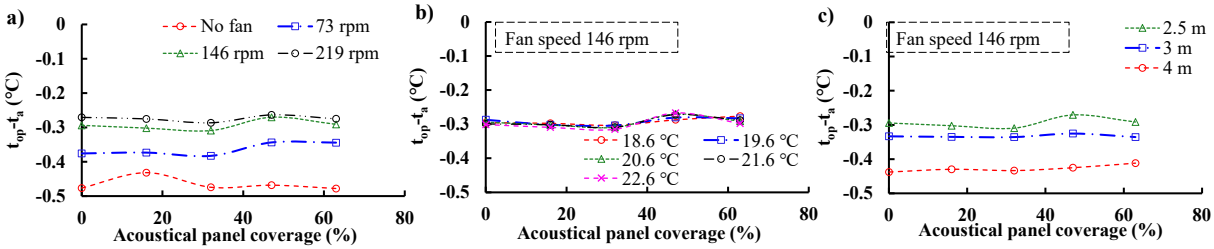

Fig. 8. a) - c) Difference between average air and operative temperature at 1.1 m height for different conditions shown in Table 1.

3.2.2 Indoor thermal comfort

Fig. 9 presents the horizontal PMV contours of Series A-D at 1.1 m height. The PMV difference of each case at 1.1 m height across the floor is within 0.5 unit. Following the air temperature distributions (Fig. 6), for the no-fan condition, the PMV value increases as the acoustical panel coverage ratio increases. For the low fan rotation speed (73 rpm), when the acoustical panel coverage is up to 47% or 63%, the PMV increases. When the acoustical panel coverage is 32% or lower, it does not have an effect on the PMV. As the fan speed increases (146 rpm and 219 rpm), the acoustical panel coverage ratio does not affect the PMV. The last row in Fig. 9 shows that the lowest PMV values occur at the highest fan rotation speed at 1.1 m height. The lower PMV at 219 rpm is due to both the increased convective heat transfer from the radiant ceiling, reducing the air temperature, and the increased air speeds in the occupied zone (see Fig. 5-6).

Fig. 10 delineates the average PMV/PD in the occupied zone versus the coverage ratio of acoustical panels, for different fan rotational speed, radiant surface temperature and room height. The average PMV increased slowly with increasing the acoustical panel coverage ratio, while the PD reduced slowly as the acoustical panel coverage ratio increases. This is attributable to the air speed in the occupied zone that decreases with increasing the acoustical panel coverage ratio, and air temperature that increases with increasing the acoustical panel coverage ratio (see Fig. 7). For the influence of fan rotational speed, Fig. 10a shows that the PMV is reduced with the fan speed, but that the low speed (73 rpm) creates an insignificant effect (0.1 unit PMV reduction from the no-fan condition). The other rotation speeds created a measurable effect, 0.4 – 0.7 PMV unit reductions from the no-fan condition. Fig. 10d shows that

the PD is augmented with the fan speed. Fig. 10d also shows that the PD of cases at highest fan speed (219 rpm) not exceeds the limit of 20%. This result indicates that a draft sensation could be encountered by the occupant owe to the large speed and cold airflow (see Fig. 5 and Fig. 6) induced by the combined system. Thus, the maximum fan speed could be adjusted near medium speed (146 rpm) to guard against the draft risk.

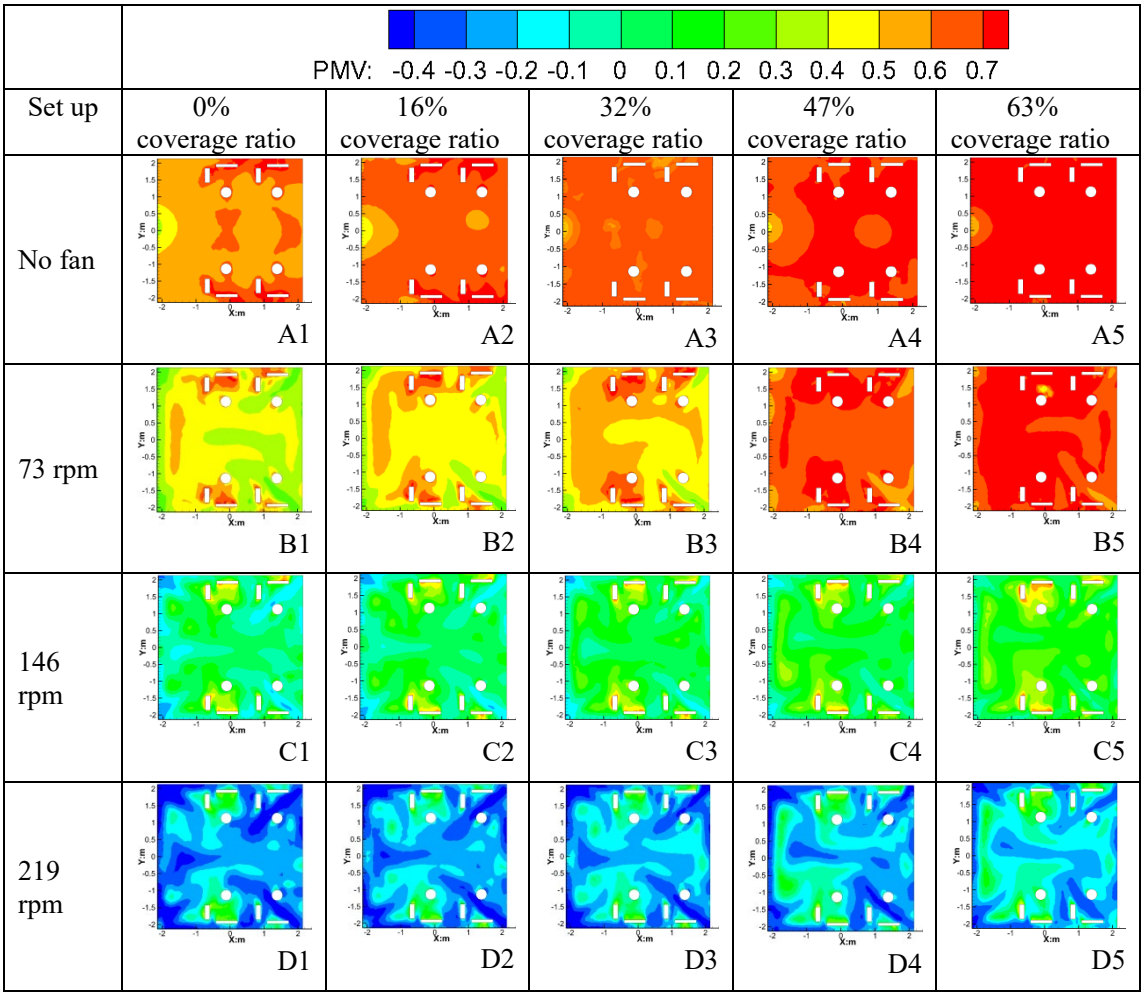

Fig. 9. Horizontal PMV contours at 1.1 m height.

Fig. 10b illustrates that the PMV grows with the increase of t_s linearly. Meanwhile, the PD reduces with the increase of radiant surface temperature linearly (Fig. 10e). It also can be found that the PMV and PD of cases (t_s = 21.6 ℃) are within the limit (-0.5 ⩽ PMV ⩽ 0.5, PD ⩽ 20%) in ASHRAE 55-2017 [24]. It demonstrated that the base radiant surface temperature (t_s = 19.6 ℃) can be raised by 2 ℃ under the medium fan speed. It indicates that upward ceiling fan is a worthwhile method allowing the radiant surface temperature to be raised, thus reduce the risk of condensation while maintain thermal comfort. Fig. 10c shows that the PMV is slightly increased with the room height, while Fig. 10f reveals that the PD is slight decreased

doi.org/10.1016/j.enbuild.2023.113492
escholarship.org/uc/item/0w2289kw

with the room height. Because of the air velocity in the occupied zone is decreased with the room height. In general, Fig. 10 demonstrates that the fan speed and radiant surface temperature have stronger impacts on the thermal comfort compared to the room height.

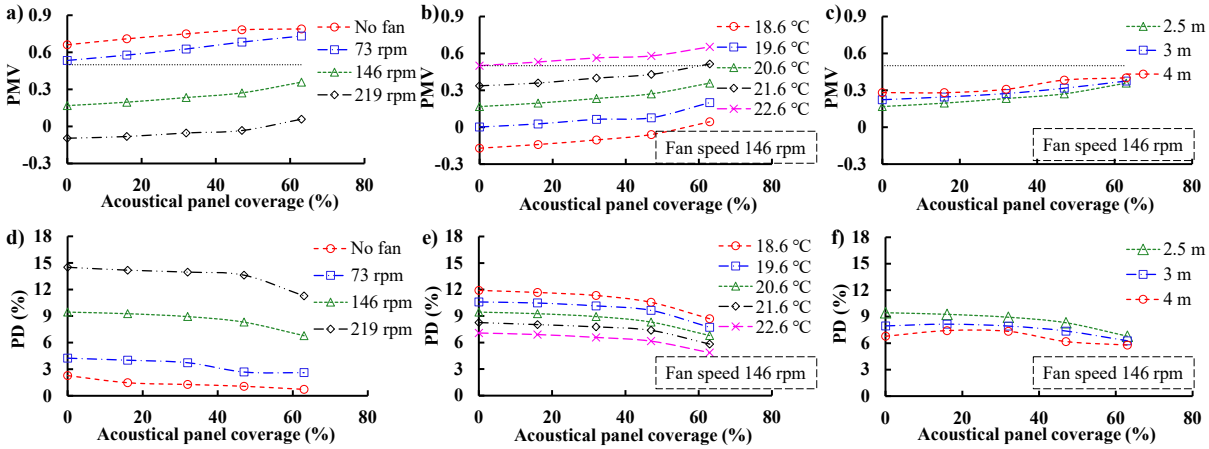

Fig. 10. Average PMV under different: a) fan rotational speed, b) radiant surface temperature and c) room height; Average PD in the occupied zone under different: d) fan rotational speed, e) radiant surface temperature and f) room height in the occupied zone.

3.3 Heat transfer performance

Figs. 11-12 reflect the heat transfer properties of radiant ceiling. Fig. 11 presents the radiative and convective heat flux versus the coverage ratio of acoustical panels, under different fan rotational speed, radiant surface temperature and room height. As the coverage of acoustical panels increased, the radiant heat fluxes are significantly reduced for all cases. The value of radiative heat flux also decreases with increasing fan speed, while the convective heat flux increases with increasing fan speed (Fig. 11a). As Fig. 11 b and c show, under the mid fan speed (146 rpm), the radiant surface temperature and room height have little effect on the value of radiative and convective heat flux.

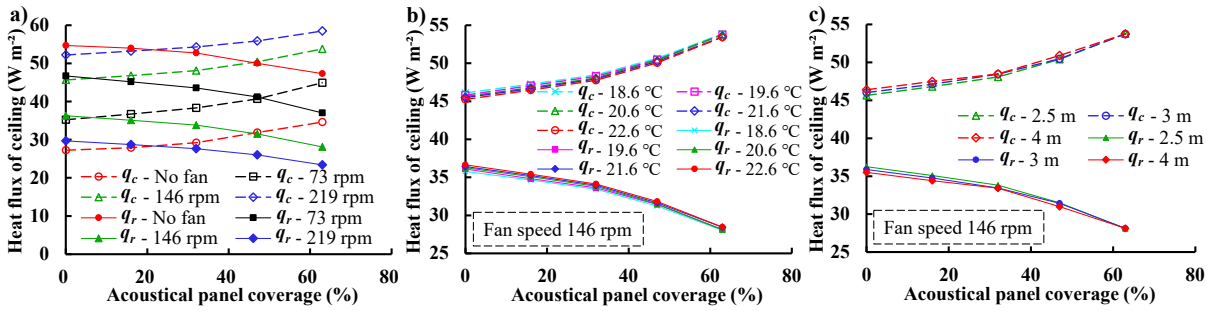

Fig. 11. Heat flux from the radiant ceiling surface for different: a) fan rotational speed, b) radiant surface temperature, c) room height.

Table 2 compares the simulated heat transfer coefficients of the radiant cooling ceiling (case A1) and the measured data given in literatures [32, 34-36]. The

simulated h_c is lower about 2.7-14.9% than measured data [34]. It might be due to the window in the experimental study [34], which enhances the natural convection. The difference between simulated h_r and literature values is within 5.6%. Compared to Cholewa et al. [32], the difference of h_{total} is within 9.8%. In general, the simulated heat transfer coefficients are consistent with the literature [32, 34-36]. These comparison results suggest that the CFD model and numerical methods are acceptable.

Table 2. Literatures and simulated heat transfer coefficients of the radiant cooling ceiling.

h_c (W m^{-2} K^{-1})		h_r (W m^{-2} K^{-1})		h_{total} (W m^{-2} K^{-1})	
simulated values	4.1	simulated values	5.3	simulated values	10.18
Causone et al. [34]	4.2-4.7	Causone et al. [34]	5.6	Cholewa et al. [32]	9.19-10
		Olesen et al. [35, 36]	5.5		

Fig. 12 illustrates the h_c, h_r and h_{total} versus the acoustical panel coverage ratio for different conditions. As Fig. 12 a-c show, the acoustical panel coverage rate, radiant surface temperature and room height has little impact on the value of h_c. The difference is within 0.3-0.5 W m^{-2} K^{-1} under a fixed fan speed. Since these factors have little effect on the airflow distribution (see Fig. 5). While h_c increases with increasing fan rotational speed. Compared to the corresponding cases without fan, the value of h_c increases by 29-48%, 126-157% and 217-255% with fan speed at 73, 146 and 219 rpm, respectively (see Fig. 12a). The higher fan rotational speed results in higher velocity gradients and thinner thermal boundary layer.

Contrary to h_c, Fig. 12 d-f illustrate that the acoustical panel coverage ratio has a stronger impact on the h_r than does the fan speed, radiant surface temperature and room height. The value of h_r decreases with increasing acoustical panel coverage rate, because the radiant heat exchange are shaded by the acoustic panels. Fig. 12d clear show that the h_r of cases with fan is lower than the case without fan at zero acoustical panel coverage, due to the radiant heat exchange from the radiant ceiling are also shaded by the ceiling fan. Compared to the corresponding case without acoustical panel, the value of h_r decreases by 25% (~1.1 W m^{-2} K^{-1}) with coverage rate at 63%. The fan rotational speed, radiant surface temperature and room height have little influence on the radiation heat transfer, the difference is within 0.3 W m^{-2} K^{-1}.

Figs. 12 g-i show that the value of h_{total} decreases with increasing acoustical panel coverage rate. Compared to the corresponding case without acoustical panel, the

doi.org/10.1016/j.enbuild.2023.113492
escholarship.org/uc/item/0w2289kw

reduction rate of h_{total} is 31.2% with coverage rate at 63%. Reduction is small (less than 10%) when the acoustical panel coverage does not exceed 32%. The reason is that the acoustical panels also have heat exchange with radiant ceiling and they then function as radiant ceiling, with some higher temperatures than the radiant ceiling. The h_{total} increases with increasing fan rotational speed. Compared to the corresponding cases without fan, the value of h_{total} increases by 40.7%, 110.0% and 176.0% with fan speed at 73, 146 and 219 rpm and coverage rate at 63%, respectively (see Fig. 12g). The value of h_{total} increases by 20.5%, 63.4% and 106.2% with fan speed at 73, 146 and 219 rpm over the no-fan base case A1 (no acoustical panels), respectively. As well as the h_c and h_r, the impact of radiant surface temperature on the h_{total} can be ignored (see Fig. 12h). Fig. 12i shows that the h_{total} is slight decreased with the room height, the difference is within 0.8% - 3.8%. In general, the sequence of four factor's effects on the h_{total} from strong to weak are fan speed, acoustical panel coverage rate, room height and radiant surface temperature.

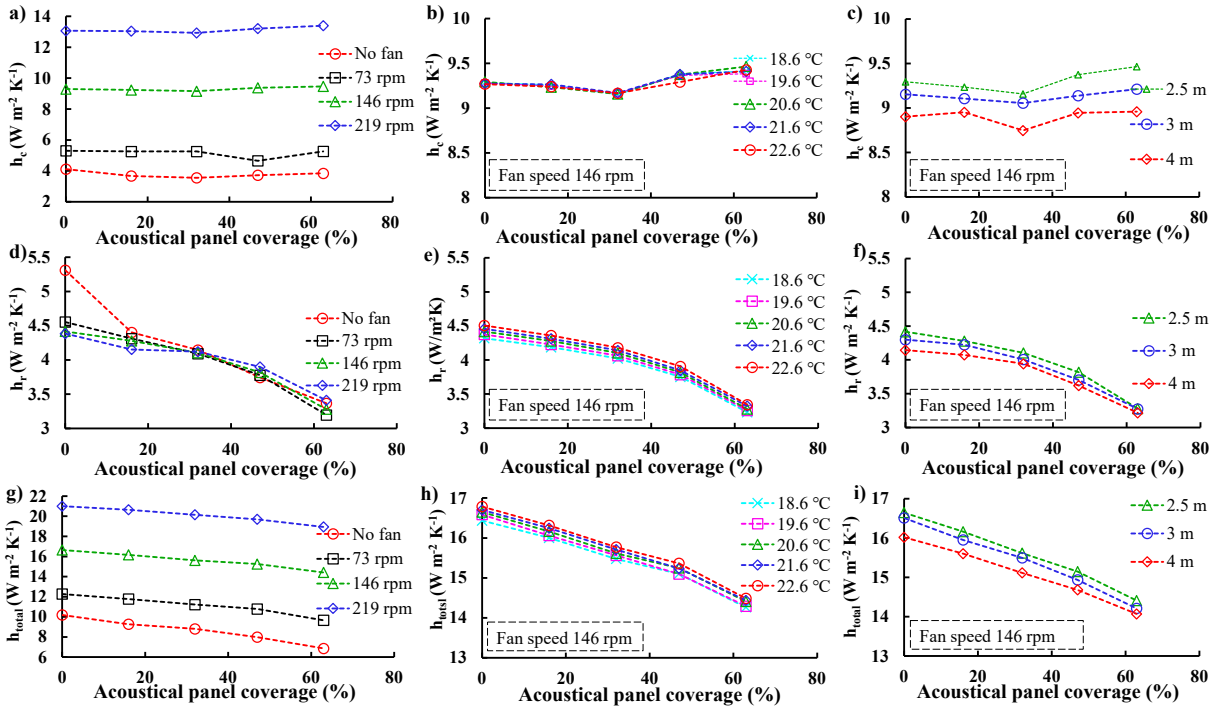

Fig. 12. Convective heat transfer coefficient under different: a) fan rotational speed, b) radiant surface temperature and c) room height; radiation heat transfer coefficient for different: d) fan rotational speed, e) radiant surface temperature and f) room height; total heat transfer coefficient for different: g) fan rotational speed, h) radiant surface temperature and i) room height.

4 Discussion

In order to verify the plausibility of this simulation study, we made a simplified estimation of the impact of acoustical panel on the radiant ceiling heat exchange, using the radiation shielding theory [37]. This theory applies to infinitely parallel surfaces, where a third surface is applied between these two surfaces (see Fig. 13).

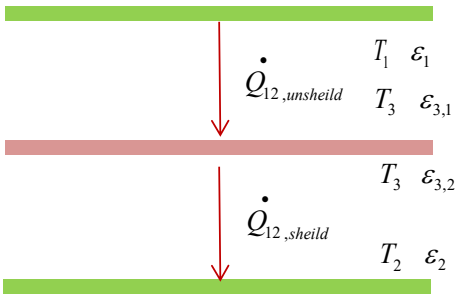

Fig. 13. The third surface is placed between two parallel panels.

If the view factor is equal to 1 and the emissivity of all surfaces is the same, then the $Q_{12,sheild}$ can be express using the following equation.

$$Q_{12,sheild} = \frac{1}{2} Q_{12,unsheild} \tag{11}$$

We make the following simplified assumptions: 1) the radiation heat exchange for the ratio of cold ceiling shaded by acoustic panels is reduced by half. 2) The total heat exchange of cold ceiling not covered by acoustic panels is unchanged. 3) The convection heat exchange does not change with the acoustical panel coverage rate (see Figs. 11 a-c). Compared with the base case without acoustical panel, the heat transfer of cold ceiling partially shielded by acoustical panels can be estimated as follows:

$$Q_{t,shaded} = \frac{A_{unshaded}}{A_{total}} Q_{total} + \frac{A_{shaded}}{A_{total}} \left(\frac{Q_r}{2} + Q_c \right) \tag{12}$$

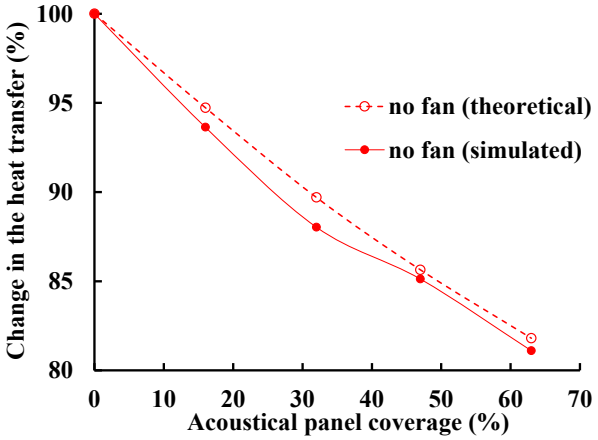

Fig. 14. Heat flux reduction due to the acoustic panels estimated with the CFD simulations

and simplified method.

Fig. 14 shows the heat transfer changes for the cases without fan, starting with acoustical panel coverage at zero. As it can be seen in Fig. 14, up to the case with 63% of the ceiling covered by acoustical panels, the simplified method adequately estimates the reduction in heat transfer due to the acoustical panels for the cases without fan. As can be expected, the radiant heat exchange is reduced with increasing the acoustical panel coverage ratio, leading to a larger heat transfer reduction. The assumption of not change in the convection heat transfer become weaker and weaker as the percent of coverage approach 100%. In fact if we consider the unlikely event that coverage rate at 100%, based on the simplified method the heat transfer compared to the unshaded case is as lower as 70%.

Through the results, it can be found that the upward ceiling fan can bring several positive effects. 1) It allows the installation of acoustical panels with higher coverage rate, improving the acoustical comfort of the office. Meanwhile, increasing the heat transfer coefficient of radiation cooling system (see Fig. 12). 2) It can be used to elevate air movement under the limit in ASHRAE 55-2017 [24], but also make the air temperature more uniform and cooler in the occupied area (see Figs. 5 and 6). It allows an increase in radiant surface temperature and being able to control the environment at a higher temperature, save energy and reduce the risk of condensation while maintain thermal comfort (see Figs. 8 and 9).

A few limitations and future perspectives need to be mentioned in this study.

Due to the upward-directed ceiling fan can bring a higher cooling capacity of the radiant cooling ceiling than the downward-directed ceiling fan [25], so this study only considers the upward-directed ceiling fan. While, our previous study [24] found that the downward-directed ceiling fan brings higher air movement than the upward-directed ceiling fan at the same fan speed in the occupied zone, it can be inferred that the comfort temperature could be raised higher than the upward-directed ceiling fan when using downward-directed ceiling fan. Thus, it would be interesting to study the influence of downward-directed ceiling fan flow on the combined system of radiant cooling ceiling and acoustical panels in the future. According to Fig. 5 and our previous studies [19, 27], ankle draft might be a potential concern, especially with downward-directed ceiling fan [19, 27]. It would be useful to evaluate the system in a climatic chamber with human subjects as done in [38] to fully investigate the system's full potential. It is also interesting to investigate the effect of ceiling fan on the cooling performance of underfloor cooling system, since the underfloor cooling system generates a large vertical air temperature gradient within the room [39].

In order to simplify the geometry model, the radiant ceiling surface temperature is simulated at a fixed temperature. Although the radiant ceiling was also simplified in many previous studies [12, 18], the panel surface may show non-uniform temperature difference. For example, Võsa et al. [39] found that the radiant ceiling surface temperature difference between two panels is within 1 °C, and the difference between the minimum and average surface temperature of a panel is within 0.5 °C. In the future, it would be necessary to perform direct simulations for the cold water

circulation pipes of the radiant ceiling [40] interacting with the ceiling fan. The condensation risk of the combined system is also worthy of further exploration.

This study principally investigated the indoor environment and heat transfer changes in the interaction between radiant ceiling panels and ceiling fan under four influencing factors: coverage ratio of acoustical panels, fan rotational speed, radiation panel temperature and room height. While some other influencing factors need to be further determined to propose the design guidelines. For example, the influence of acoustical panel coverage patterns could be studied as well, since Domínguez et al. [9] reported that vertically suspended acoustical panels have less impact on ceiling cooling performance than horizontal acoustical panels. The distance between the radiant ceiling and acoustic clouds is also needs to be explored, since the airflow passing through narrow air gaps could increase the air velocity and convective heat transfer rate. Besides, the distance between the radiant ceiling and ceiling panel also can be a major factor on the cooling performance of an open type radiant cooling system [18] interacting with ceiling fan. In addition, the cooling load of the wall and window also need to be considered for designing this combined system in the practical application. Furthermore, to comprehensively evaluate this combined system, it is also necessary to explore its energy and economic performance. The use of ceiling fan at medium speed allows an increase in radiant surface temperature and being able to control the environment at a higher temperature while maintain thermal comfort (see Figs. 9 and 10). It indicated that energy consumption reduces as fan speed increases, but the PD and noise would rise with the increment of fan speed. Hence, in order to get the compromise between energy consumption and thermal comfort, the statistical multi-objective optimization study considering the influence factors mentioned above should be further conducted, then optimized design guidelines and control strategies accordingly.

5 Conclusions

This study systematically investigated the indoor environment and heat transfer changes in the interaction between radiant ceiling panels, acoustical panels, and ceiling fan. A validated CFD simulation model was employed to determine the impact of ceiling fan speed, panel surface temperature, ceiling height, in addition to acoustic cloud coverage ratio. The following conclusions are noteworthy.

1) The air velocity in the occupied zone is augmented with the fan speed. While the air temperature, operative temperature and temperature non-uniformity are reduced with increasing the fan speed. An upward-directed ceiling fan reduces the average air and operative temperature by 2-6 ℃ in the occupied zone. The acoustical panel coverage ratio has little influence on the airflow pattern and air speed, but the air and operative temperature increase as the acoustical panel coverage ratio increases.
2) Fan speed, acoustical panel coverage ratio and radiant surface temperature have a stronger effect on the PMV than does the room height. The PMV increased with increasing the acoustical panel coverage ratio and radiant surface temperature, and

doi.org/10.1016/j.enbuild.2023.113492
escholarship.org/uc/item/0w2289kw

decreased with the fan speed. The fan speed at the low level (73 rpm) it is too small to create enough impact on thermal sensation; the medium and high fan speeds (146 and 219 rpm) can create measurable effects on PMV. The base radiant surface temperature (19.6 ℃) can be raised by 2 ℃ under the medium fan speed while maintain thermal comfort. Fans allow increasing the radiant surface temperature and controlling the environment at a higher temperature, then save energy and avoid condensation.

3) The convective heat transfer coefficient dramatically increases with increasing fan rotational speed, while the other influencing factors are insignificant. The radiation heat transfer coefficient reduces with increasing acoustical panel coverage rate, decreases by 25% with coverage rate at 63%. The total heat transfer coefficient of radiant ceiling increases with fan speed up to 106.2% over a no-fan base case, and decreases with increased acoustical panel coverage ratio. The fan can fully compensate for the radiant heat exchange reduction due to the acoustical panels. Besides, the impact of room height and radiant surface temperature on the heat transfer coefficient is insignificant.
4) In the future, other possible influencing parameters on the thermal and heat transfer performance of the combined system also need to be identified. The draft and condensation risk of the combined system is also worthy of further exploration. In addition, in order to get the compromise between energy consumption and thermal comfort, the statistical multi-objective optimization study considering the main influence factors should be further conducted, then optimized design guidelines and control strategies accordingly.

ACKNOWLEDGMENT

The research was supported by the National Natural Science Foundation of China (No. 52268019) and the California Energy Commission (CEC) Electric Program Investment Change (EPIC) (Grant Award #: EPC-16-013).

References

[1] https://www.iea.org/reports/buildings.

[2] Y. Zhou, Climate change adaptation with energy resilience in energy districts—A state-of-the-art review, Energy Build. 279 (2023) 112649.

[3] W. Jung, F. Jazizadeh, Human-in-the-loop HVAC operations: A quantitative review on occupancy, comfort, and energy-efficiency dimensions, Appl. Energ. 239 (2019) 1471-1508.

[4] C. Karmann, S. Schiavon, L.T. Graham, P. Raftery, F. Bauman, Comparing temperature and acoustic satisfaction in 60 radiant and all-air buildings, Build. Environ. 126 (2017) 431-441.

[5] C. Karmann, S. Schiavon, F. Bauman, Thermal comfort in buildings using radiant vs. all-air systems: A critical literature review, Build. Environ. 111 (2017) 123-131.

[6] Y. Wang, X. Wu, J. Gao, A. Feng, J. Wang, D. Liu, X. Zhou, Simplified model for heat transfer and surface temperature of prefabricated radiant heating and cooling system, Energy Build. 276 (2022) 112522.

[7] C. Karmann, F.S. Bauman, P. Raftery, S. Schiavon, W.H. Frantz, K.P. Roy, Cooling capacity and acoustic performance of radiant slab systems with free-hanging acoustical clouds, Energy Build. 138 (2017) 676-686.
[8] P. Weitzmann, E. Pittarello, B.W. Olesen, The cooling capacity of the thermoactive building system combined with acoustic ceiling, in: Nordic Symposiumon Building Physics 2008, Copenhagen, Denmark, 2008.
[9] L.M. Domínguez, O.B. Kazanci, N. Rage, B.W. Olesen, Experimental and numerical study of the effects of acoustic sound absorbers on the cooling performance of Thermally Active Building Systems, Build. Environ. 116 (2017) 108-120.
[10] B. Köhler, N. Rage, P. Chigot, C.A. Hviid, Thermo-active building systems and sound absorbers: Thermal comfort under real operation conditions, Build. Environ. 128 (2018) 143-152.
[11] M. Dawe, C. Karmann, S. Schiavon, F. Bauman, Field evaluation of thermal and acoustical comfort in eight North-American buildings using embedded radiant systems, PloS one 16(10) (2021) e0258888.
[12] C. Zhang, M. Pomianowski, P.K. Heiselberg, T. Yu, A review of integrated radiant heating/cooling with ventilation systems- Thermal comfort and indoor air quality, Energy Build. 223 (2020) 110094.
[13] B. Ning, Y. Chen, H. Liu, S. Zhang, Cooling capacity improvement for a radiant ceiling panel with uniform surface temperature distribution, Build. Environ. 102 (2016) 64-72.
[14] A. Novoselac, B.J. Burley, J. Srebric, New Convection Correlations for Cooled Ceiling Panels in Room with Mixed and Stratified Airflow, HVAC&R Res. 12(2) (2006) 279-294.
[15] M. Ye, A.A. Serageldin, K. Nagano, Numerical optimization of a novel ceiling radiant cooling panel combined with wall attached ventilation system, Case Stud. Therm. Eng. 26 (2021) 101066.
[16] M.K. Kim, J. Liu, S.-J. Cao, Energy analysis of a hybrid radiant cooling system under hot and humid climates: A case study at Shanghai in China, Build. Environ. 137 (2018) 208-214.
[17] W. Zhao, S. Kilpeläinen, R. Kosonen, J. Jokisalo, S. Lestinen, Y. Wu, P. Mustakallio, Human response to thermal environment and perceived air quality in an office with individually controlled convective and radiant cooling systems, Build. Environ. 195 (2021) 107736.
[18] J.-S. Choi, G.-J. Jung, K.-N. Rhee, Cooling performance evaluation of a fan-assisted ceiling radiant cooling panel system, Energy Build. 281 (2023) 112760.
[19] W. Chen, H. Zhang, E. Arens, M. Luo, Z. Wang, L. Jin, J. Liu, F.S. Bauman, P. Raftery, Ceiling-fan-integrated air conditioning: Airflow and temperature characteristics of a sidewall-supply jet interacting with a ceiling fan, Build. Environ. 171 (2020) 106660.
[20] Y. Zhai, C. Elsworth, E. Arens, H. Zhang, Y. Zhang, L. Zhao, Using air movement for comfort during moderate exercise, Build. Environ. 94 (2015) 344-352.
[21] Y. Zhai, Y. Zhang, H. Zhang, W. Pasut, E. Arens, Q. Meng, Human comfort and perceived air quality in warm and humid environments with ceiling fans, Build. Environ. 90 (2015) 178-185.
[22] J. Guenther, O. Sawodny, Feature selection and Gaussian Process regression for personalized thermal comfort prediction, Build. Environ. 148 (2019) 448-458.
[23] H. Zhang, E. Arens, Y. Zhai, A review of the corrective power of personal comfort systems in non-neutral ambient environments, Build. Environ. 91 (2015) 15-41.
[24] ASHRAE Standard 55–2017 Thermal Environmental Conditions for Human Occupancy, Atlanta, GA: American Society of Heating, Ventilation, Refrigerating and Air Conditioning

Engineers, (2017).
[25] C. Karmann, F. Bauman, P. Raftery, S. Schiavon, M. Koupriyanov, Effect of acoustical clouds coverage and air movement on radiant chilled ceiling cooling capacity, Energy Build. 158 (2018) 939-949.
[26] S. Zhu, J. Srebric, S.N. Rudnick, R.L. Vincent, E.A. Nardell, Numerical Modeling of Indoor Environment with a Ceiling Fan and an Upper-Room Ultraviolet Germicidal Irradiation System, Build. Environ. 72 (2014) 116-124.
[27] W. Chen, S. Liu, Y. Gao, H. Zhang, E. Arens, L. Zhao, J. Liu, Experimental and numerical investigations of indoor air movement distribution with an office ceiling fan, Build. Environ. 130 (2018) 14-26.
[28] J. Hu, Y. Kang, Y. Lu, J. Yu, H. Li, K. Zhong, Numerical investigation of the thermal and ventilation performance of a combined impinging jet ventilation and passive chilled beam system, Build. Environ. 226 (2022) 109726.
[29] ISO, ISO 7730: 2005, Ergonomics of the Thermal Environment and Analytical Determination and Interpretation of Thermal Comfort Using Calculation of the PMV and PPD Indices and Local Thermal Comfort Criteria, 2005 (Geneva, Switzerland).
[30] S.Y. Qin, X. Cui, C. Yang, L.W. Jin, Thermal comfort analysis of radiant cooling panels with dedicated fresh-air system, Indoor Built Environ. 30(10) (2020) 1596-1608.
[31] O. Acikgoz, O. Kincay, Experimental and numerical investigation of the correlation between radiative and convective heat-transfer coefficients at the cooled wall of a real-sized room, Energy Build. 108 (2015) 257-266.
[32] C. Tomasz, A. Rafał, S.-O. Alicja, A. Mariusz, On the heat transfer coefficients between heated/cooled radiant ceiling and room, Appl. Therm. Eng. 117 (2017) 76-84.
[33] M.R. Krusaa, I. Hoffmann, C.A. Hviid, Experimental investigation of integrated radiant ceiling panel and diffuse ceiling ventilation under cooling conditions, Energy Build. 266 (2022) 112101.
[34] F. Causone, S.P. Corgnati, M. Filippi, B.W. Olesen, Experimental evaluation of heat transfer coefficients between radiant ceiling and room, Energy Build. Vol.41(No.6) (2009) 622-628.
[35] B.W. Olesen, E. Michel, F. Bonnefoi, M. De Carli, Heat exchange coefficient between floor surface and space by floor cooling: theory or a question of definition, ASHRAE Trans. 106 (2000) 684.
[36] B.W. Olesen, M. Koschenz, C. Johansson, New European Standard Proposal for Design and Dimensioning of Embedded Radiant Surface Heating and Cooling Systems, ASHRAE Trans. 109 (2003) 656-668.
[37] A. Bejan, Heat transfer: Evolution, design and performance, John Wiley & Sons (2022).
[38] T. Arghand, A. Melikov, Z. Bolashikov, P. Mustakallio, R. Kosonen, Individually controlled localized chilled beam with background radiant cooling system: Human subject testing, Build. Environ. 218 (2022) 109124.
[39] K.-V. Võsa, A. Ferrantelli, J. Kurnitski, Cooling Thermal Comfort and Efficiency Parameters of Ceiling Panels, Underfloor Cooling, Fan-Assisted Radiators, and Fan Coil, Energies 15(11) (2022) 4156.
[40] D. Xie, Y. Wang, H. Wang, S. Mo, M. Liao, Numerical analysis of temperature non-uniformity and cooling capacity for capillary ceiling radiant cooling panel, Renew. Energ. 87 (2016) 1154-1161.